Microstructural evaluation and characterization of solid-state reaction of B_2O_3 doped $BaZr_xTi_{1-x}O_3$ ceramics

Kerim Emre Öksüz[1], Şaduman Şen[2] and Uğur Şen[2]

1) Cumhuriyet University, Department of Metallurgical & Materials Engineering, 58140, Sivas, Turkey.
2) Sakarya University, Department of Metallurgical & Materials Engineering, 54187, Sakarya, Turkey.

Email: kerimemreoksuz@gmail.com

Available Online at: www.austceram.com/ACS-Journal

Abstract
0.5 wt. % B_2O_3 doped $BaZr_xTi_{1-x}O_3$ ceramics (x = 0, 0.1, 0.2, 0.3, 0.4) were synthesized by adapting the solid-state synthesis method. B_2O_3 used as a sintering additive in the BT and BZT ceramics can vaporize easily at high temperatures, so it can be adopted as a vapor dopant. The influence of the substitution content on the crystallographic structure, phase transition, grain size, microstructure and physical properties of BT and BZT ceramics were discussed. Materials Pro+ image analysis software was used for the measurement of grain size of piezoelectric ceramics. XRD analysis at room temperature revealed that a structural transformation from tetragonal to rhombohedral with increasing ZrO_2 content in the BT matrix. The scanning electron microscope (SEM) and energy-dispersive X-ray spectroscopy (EDS) were employed to investigate the microstructures and surface-fracture morphologies of the sintered samples. The relative densities and open porosity were measured by the Archimedes' immersion method in distilled water.

Keywords: $BaTiO_3$, barium-titanate-zirconate, sintering, grain size, microstructure, domain

INTRODUCTION

The study of ABO_3-type solid solutions based on perovskite-structured barium titanate ($BaTiO_3$) has been of great interest so far. It offers the possibility to optimize several electrical properties for the manufacture of a number of devices, including multilayer capacitors, actuators and sensors etc. [1]. Pure $BaTiO_3$ undergoes a paraelectric to ferroelectric phase transition at 130 °C, which is accompanied by a sharp peak in the permittivity curve. Isovalent dopants, such as strontium and zirconium, are often employed to shift the Curie point for particular applications. The $Ba_xSr_{1-x}TiO_3$ (BST) has a high dielectric constant, low leakage current and low dielectric dispersion against frequency [2, 3, 4, 5]. However, the leakage current often abruptly turns up in the orders of magnitude as the applied field exceeds a critical value of several hundreds kV/cm, and breakdown occurs in a field around 2 MV/cm$^{-3)}$[4]. Recently, $BaZr_xTi_{1-x}O_3$ (BZT) has been chosen as an alternative to BST in the fabrication of ceramic capacitors. The Zr^{4+} ion (0.087 nm) is chemically more stable than the Ti^{4+} (0.068 nm) and has a larger ionic size to expand the lattice. Therefore, the conduction by electron hopping between Ti^{4+} and Ti^{3+} would be depressed by the substitution of Ti with Zr [6]. Hongwei Chen et al. [7] reported the $BaZr_xTi_{1-x}O_3$ ceramics with x = 0.05, 0.10, 0.15, and 0.20 and investigated the microstructure and dielectric properties. Generally, optimization of the electrical properties of $BaTiO_3$ requires a high density and controlled microstructure. BT ceramics are sintered at temperatures between 1300-1350°C. Therefore, a great deal of research has been carried out to reduce the sintering temperature and to improve the grain growth by a liquid phase sintering either by altering the cation stoichiometry or by adding some liquid forming sintering aids. Many oxides such as Bi_2O_3, LiF, B_2O_3, SiO_2 and Al_2O_3 [8, 9, 10, 11, 12] have been used for the formation of the required liquid phase to enhance densification and grain growth in the BT based ceramics. Qi et al. [13] focused their attention on the dielectric properties of barium titanate ceramics doped by B_2O_3 vapor. B_2O_3 has rarely caused attention as a dopant rather than flux addition. Because B_2O_3 vaporizes easily at high temperatures, it can be adopted as a vapor dopant. In donor doped $BaTiO_3$ ceramics, the B_2O_3 vapor dopant can improve the positive temperature coefficient resistivity effect [14, 15] distinctly and decrease the sintering temperature [16]. Ciomaga et al. [17] reported, $BaZr_xTi_{1-x}O_3$ ceramics with x = 0.10, 0.15 and 0.18 prepared by solid-state reaction were investigated and showed that the microstructure evaluation. The main objective of the study was to investigate the microstructural

© Copyright 2015, The Australian Ceramic Society ISSN 0004-881X

evaluation, domain structure and physical properties of B_2O_3 doped $BaZr_xTi_{1-x}O_3$ ceramics (x = 0, 0.10, 0.2, 0.3 and 0.4).

METHODS AND PROCEDURES

$BaZr_xTi_{1-x}O_3$ (x=0-0.4) ceramics were prepared by solid-state reaction using high purity $BaCO_3$ (1 µm, ≥ 99.9%), TiO_2 (0.5 µm, ≥99.9%), H_3BO_3 (1 µm, ≥99.5%) 99.9% and ZrO_2 (0.5 µm, ≥99.5%) (Alfa Aesar; purity ≥99.5%) powders in a Nalgene bottle with an aqueous dispersion (ethyl alcohol). The slurry was milled overnight and then dried in a Pyrex pan. The powder was calcined in O_2 at 950 °C for 2 h. The final powder was attrition milled for 10 h and then sieved to less than 45 µm prior to being mixed with an organic binder (5% PVA 72000 g/mol) and 0.5 wt. % B_2O_3. Pellets were pressed uniaxially at 100 MPa and sintered at 1350 °C for 4 h in static air in a closed alumina crucible and cooled down to room temperature (at a ramp of 5°C/min.). The relative density and porosity of the samples were measured by Archimedes' method. The vacuum method (ISO 10545-3) was used in the laboratory to determine water absorption with greater precision. The crystal structure of the samples was determined from X-ray diffraction (XRD) data. An X-ray Diffractometer (Rigaku D/MAX/2200/PC) with a monochromatic Cu-K_α radiation (λ= 1.5408 Å) was used over a 2θ angle from 20°to 80° to characterize the crystal structure of the sintered compacts. The surface-fracture morphology and elemental analysis of the ceramics was examined by using a Scanning electron microscope (SEM, Model JEOL-JSM 6060-LV, Japan) and energy-dispersive X-ray spectroscopy (EDS).

RESULTS AND DISCUSSION

The XRD patterns of BZT ceramics with various Zr/Ti ratios are shown in Fig. 1. It is proven that all the ceramics with various Zr/Ti ratios are of perovskite crystal structure. No other phases are observed in the spectra. Sharp and well defined diffraction peaks indicate that ceramics have long range crystalline order. This also clearly indicates that Zr^{4+} is dissolved in the BT lattice to form homogeneous solid solutions. The magnified patterns in the vicinity of 2θ ≈ 45°as shown in the inset of Fig. 1, depict that the (002) and (200) diffraction peaks are clearly split in $BaTiO_3$ sample. But the peaks get slip to lower 2θ values with ZrO_2 addition to be rhombohedral structure, where x= 0.1 to 0.4. At room temperature, the sample $BaZr_{0.1}Ti_{0.9}O_3$ possesses tetragonal phase, which is identified by the split (002/200) diffraction peaks at around 2θ ≈ 45°. With the increase in Zr content the phase structure of the prepared samples changes to rhombohedral phase with a single (200) peak ($BaZr_{0.4}Ti_{0.6}O_3$).

The XRD studies do not show any phases related with either B_2O_3 which indicates the low content of the boron oxide and the loss of B_2O_3 by evaporation from the structure or its presence as an amorphous phase. The average crystallite size was calculated from XRD peak broadening using the most intense three peaks (around 2θ ≈ 30°,45° and 56°) employing the Debye Scherrer equation; D= Kλ/βCosθ, where, K (constant)=0.89, β is the full width at half maxima (in radian) and θ is the Bragg's angle. The values were found to be 35 nm, 37 nm, 42 nm, 43 nm, 45nm for $BaZr_xTi_{1-x}O_3$ (x=0-0.4) ceramics, respectively.

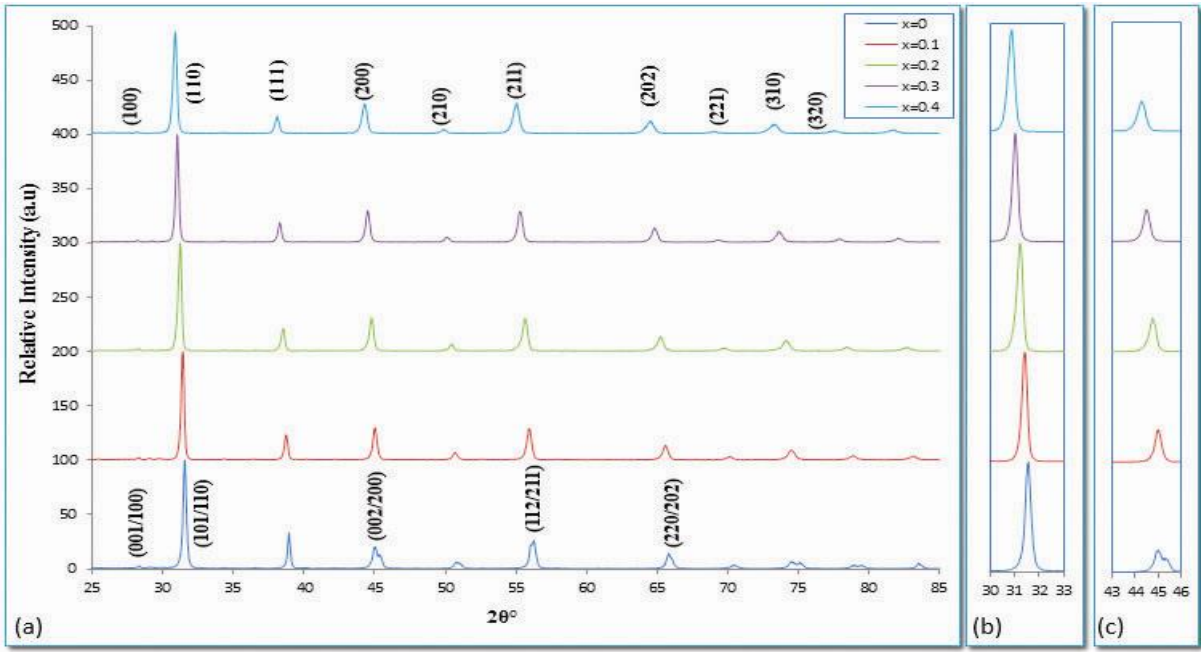


Fig. 1. (a) XRD patterns of $BaZr_xTi_{1-x}O_3$ (x=0-0.4) ceramics samples at RT; (Inset) The magnified patterns in the vicinity of 31.5°(b) and 45°(c).

The crystallite size gradually increases with the increasing ZrO_2 content. The results agree with the Sindhu et.al [18] and Vasilescu et.al [19] studies.

The SEM images of BZT ceramics are shown in Fig. 2 (a-e), respectively. By using Materials Pro+ image analysis software, the grain sizes of BZT ceramic samples had been studied. In the present study, B_2O_3 addition cannot cause a formation in any phases including boron and any amorphous structure took place in the samples microstructures. The average grain sizes of the BZT ceramics in Fig. 2(a)–(e) were ~2.43µm, ~4.65µm, ~3.08µm and ~2.87µm, 1.77 µm respectively. Le Dai Vuong et.al [20] and Choudhury et.al [21] study showed that the ZrO_2 addition caused to increase of the grain sizes o of the BT ceramics at low concentration, but the increase in ZrO_2 content causes to decrease of the grain size of BZT ceramics which agrees well with the present study.

The domain structures of $BaZr_xTi_{1-x}O_3$ ceramics with various grain sizes can be clearly seen from Fig. 2 (a-e). It can be shown from the SEM images that the Zr modified BZT ceramics exhibit fine grain size and tetragonal structure to rhombohedral structural transformation. In all the ceramics, the grains have an irregular morphology and are non-uniformly distributed with multiple grain boundaries at the surface as well as within the bulk region.

The effects of ZrO_2 addition to BT showed that a dense microstructure which is essentially consisting of small grains (average grain size ~2.43µm) was observed for pure BT. After doping 10 mol % ZrO_2 in sample $BaZr_{0.1}Ti_{0.9}O_3$, grain size increased significantly (average grain size ~ 4.65µm) as shown in Figure 2(b).

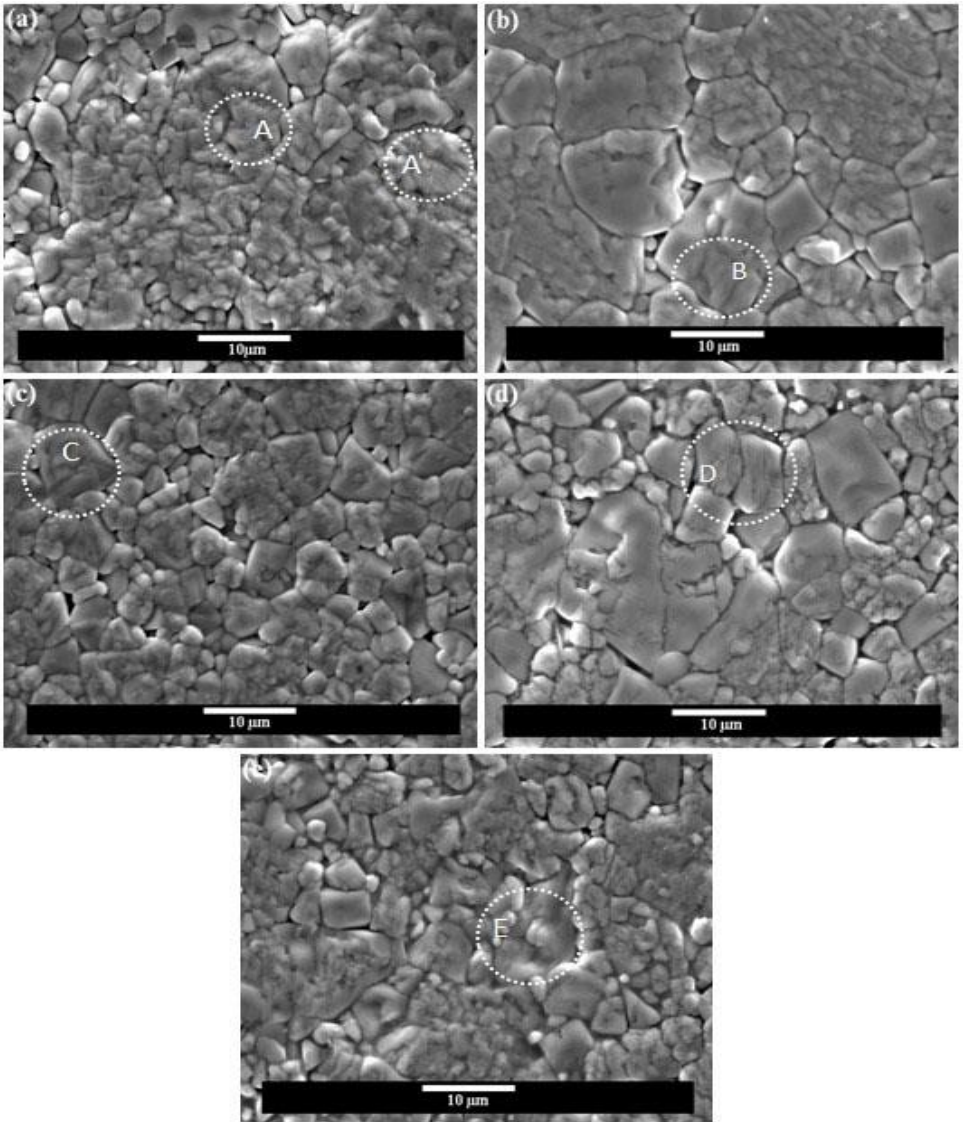


Fig. 2. SEM micrographs and domain structures of $BaZr_xTi_{1-x}O_3$ ceramics sintered at 1350 °C for 4h.
a) *x=0*, b) *x=0.1*, c) *x=0.2* d) *x=0.3* e) *x=0.4*.

These characteristics in microstructure are governed due to the matter transportation mechanism occurring during the solid state reaction [18]. All Zr doped BT grains had nearly the hexagonal shape with 120° angles as shown in Figure 2 (a-e). With the increase in Zr concentration, the fraction of large grains decreased significantly, resulting in a bimodal distribution of large grains in the fine grain matrix [22].

180°-Domains are observed in BZT ceramic samples with different grain sizes, as indicated with circles A, A', B, C, D and E in Fig. 2(a)–(e). Domain shapes of $BaZr_xTi_{1-x}O_3$ (x=0-0.4) ceramics include lamellar and "water-mark" structures. As clarified in the literature [23, 24, 25, 26], many efforts, including theoretical and experimental, have been taken to study ferroelectric domain structure in the ceramics and thin films.

-

, B and C. Domains with the lamellar feature is only observed in BZT ceramic samples, as indicated with circle D and E in Fig. 2(d) and (e). It is found that ZrO_2 content influence types of domain of $BaZr_xTi_{1-x}O_3$ (x=0-0.4) ceramics. This observation is in good agreement with the literature findings as well [26]. Some Zr rich regions were detected in microstructure from point shooting analysis of EDS spectra. Micrograph is showing that there are coarse grains as well as small grains. Fig. 3(b)-(d) shows the EDS Spectrum for pure BT and $BaZr_{0.4}Ti_{0.6}O_3$ ceramics sintered at 1350 °C for 4h and the results of compositional analysis taken from the extremely large grains and relatively small grains in Fig. 3(a)-(c).

Secondary and backscattered electron (SEM –BEI) images of microstructure of fractured ceramics are shown in Fig. 4. For compacts sintered at 1350º C, densification proceeded (Fig. 4(a)-(b)). A significant amount of necking is apparent between grains in Fig. 4(a) and (d) independent of the initial powder size and sintering conditions. Relative density and open porosity level of the sintered $BaZr_xTi_{1-x}O_3$ (x=0-0.4) bulk ceramics is shown in Fig. 5. The relative densities were measured by the immersion method in water (Archimedes') [27]. A relative density above 90% was found for all the compositions with the exception of the $BaZr_{0.4}Ti_{0.6}O_3$ samples for which it was ~88%. It is believed that the microstructural refinement accompanied by the increase of the intergranular porosity inducing a poor densification in highly Zr-doped barium titanate ceramics originate most likely in the so-called Kirkendall effect caused by the different diffusion rates of the cationic species that compose the BZT solid solutions [28].

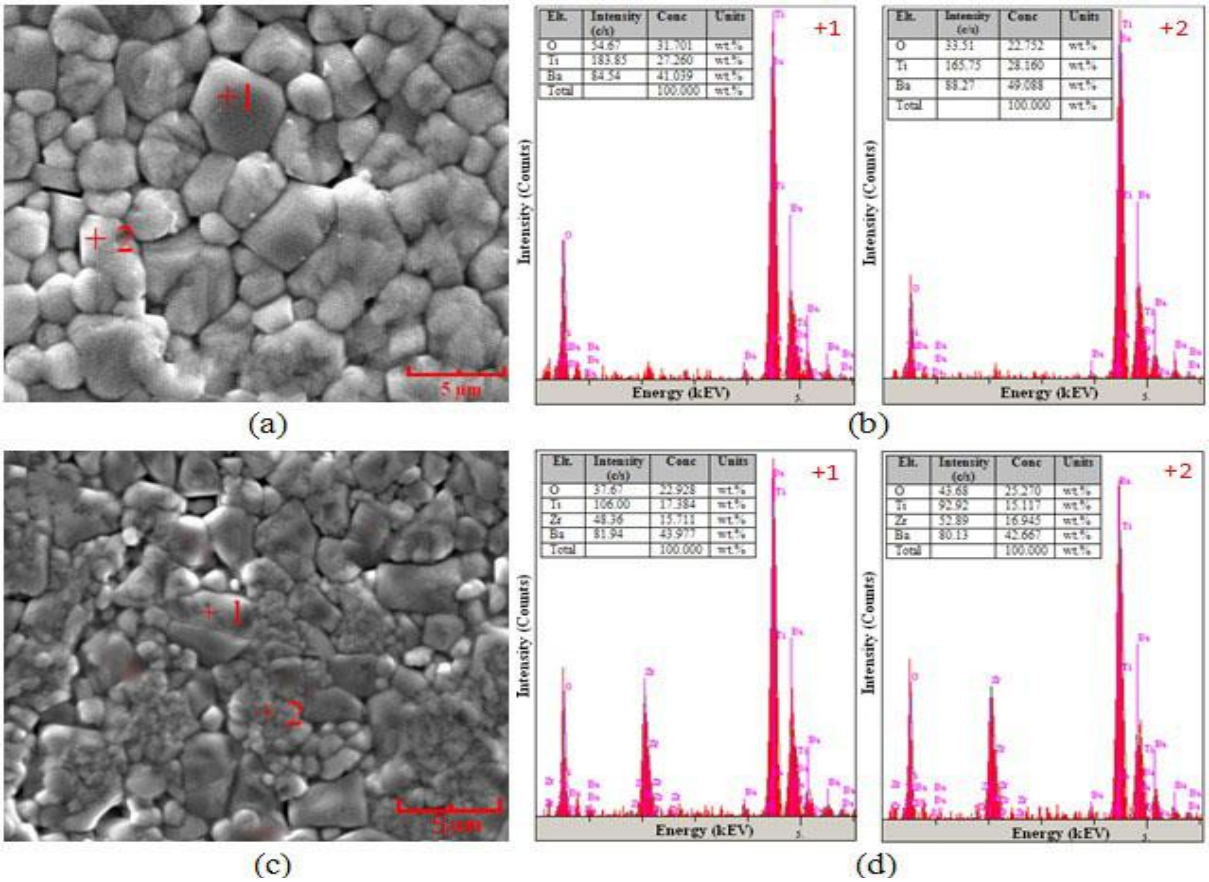


Fig 3: EDS Spectrum for pure BT and $BaZr_{0.4}Ti_{0.6}O_3$ ceramics.

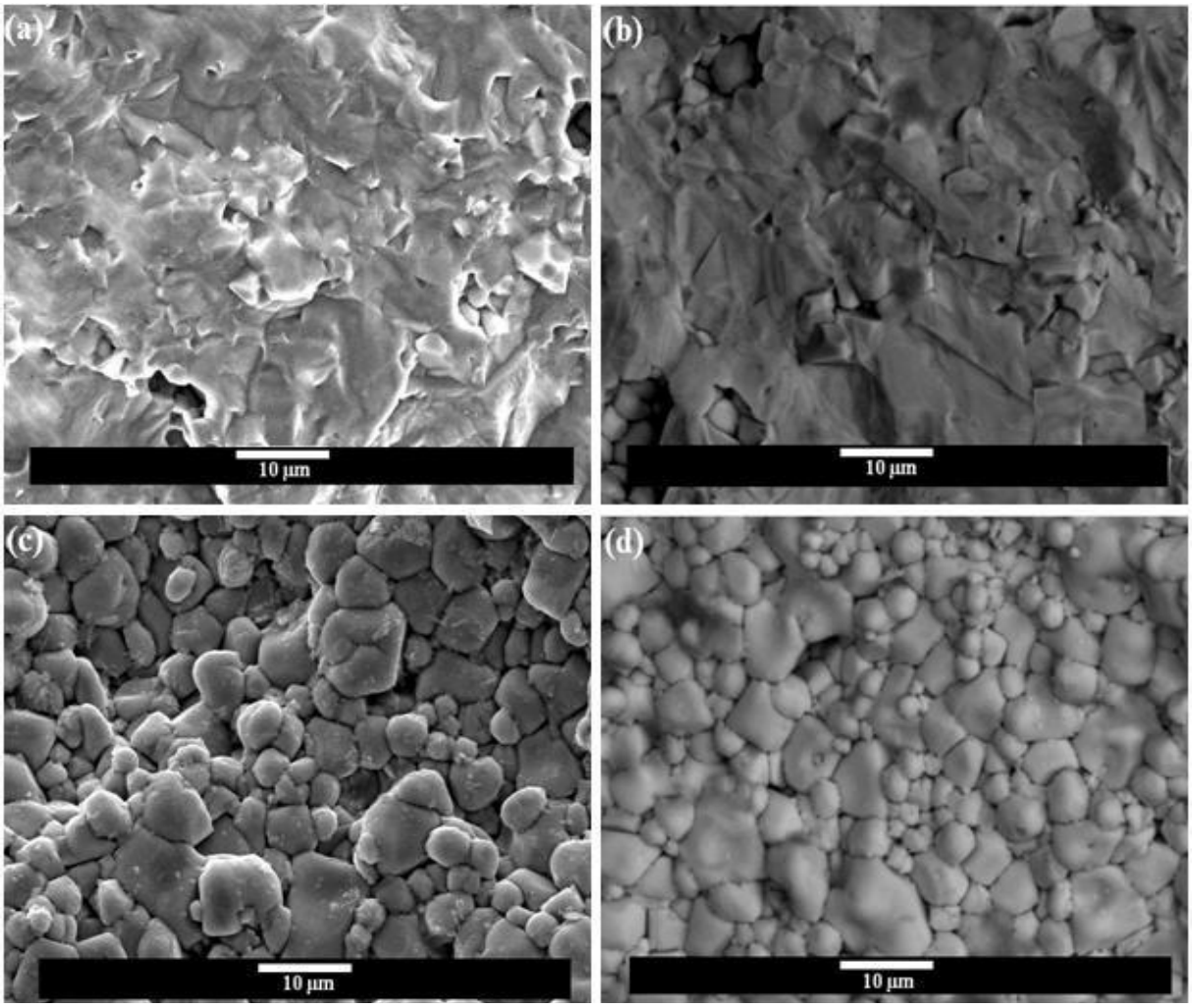


Fig. 4. SEM-BES image of the fracture surface of (a)-(b) pure BT and SEM-BES image of the fracture surface of (c)-(d) $BaZr_xTi_{1-x}O_3$ (x=0.4).

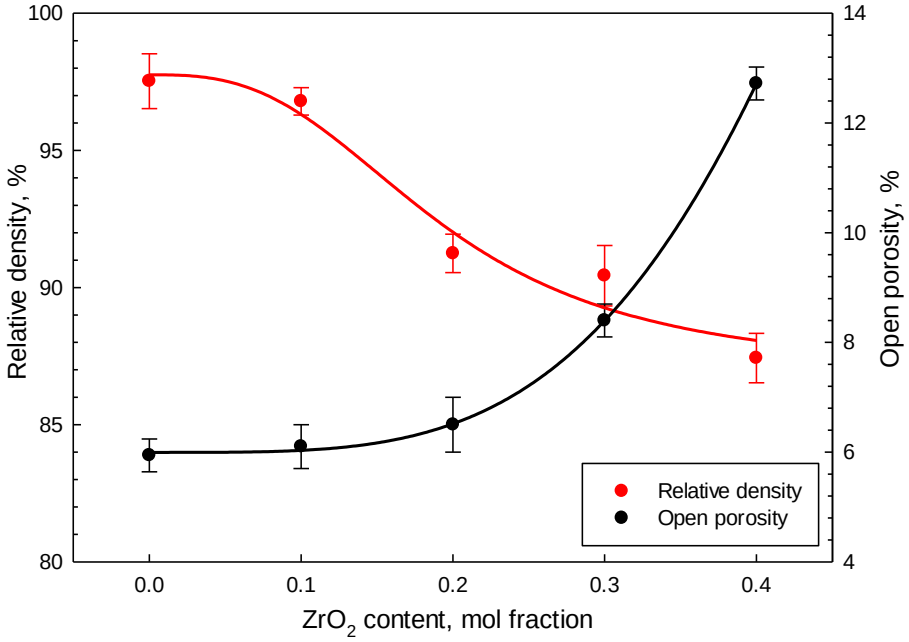


Fig. 5. Relative density versus open porosity graph of $BaZr_xTi_{1-x}O_3$ (x=0-0.4) ceramics.

CONCLUSIONS

$(Ba(Zr_xTi_{1-x})O_3$ (x=0-0.4) solid solutions were prepared by the solid state reaction method. B_2O_3 addition cannot cause to the formation of any phases including boron and any amorphous structure took place in the samples microstructures. All the BT/BZT ceramics examined showed that there was a single-phased perovskite crystal structure after sintering at 1350°C for 4 hours. The crystalline structure and microstructure of BZT ceramics are strongly depended to the Zr content. The ZrO_2 causes an increase in the grain size of the BT ceramics at low concentration, but the increase in ZrO_2 content cause to decrease of the grain size of BZT ceramics. According to SEM micrographs, it is found that addition of ZrO_2 content influences on the types of domain of BZT ceramics. Domains with lamellar and "water-mark" characters are observed. The relative density and microstructure refinement are accompanied by the subsequent increase of the intergranular porosity by Kirkendall effect.

REFERENCES

1. **J. Moulson and J. M. Herbert**, *Electroceramics: Materials, Properties and Applications*. London: Chapman-Hall; 1990.
2. **H.V. Alexandru, C. Berbecaru, A. Ioachim, M.I. Toacsen, M.G. Banciu, L. Nedelcu, D. Ghetu,** Ferroelectric solid solutions $(Ba,Sr)TiO_3$ for microwave applications, Mater. Sci. Eng. B, (2004), 149-152.
3. **B. Chen, H. Yang, J. Miao, L. Zhao, L.X. Cao, B. Xu, X.G. Qiu, B.R. Zhao,** Leakage current of $Pt/(Ba_{0.7}Sr_{0.3})TiO_3$ interface with dead layer, J. Appl. Phys., Vol.[**97**], (2005), 24-32.
4. **J.D. Baniecki, T. Shioga, K. Kurihara, N.Kamehara**, Erratum: "A study of current transport in $(Ba_xSr_{1-x})Ti_{1+v}O_3$+z thin-film capacitors containing a voltage-dependent interface state charge distribution, J. Appl. Phys., Vol.[**97**], 101-114 (2005).
5. **P. Babilo, T. Uda and S.M. Haile,** Processing of yttrium doped barium zirconate for high proton conductivity, J. Mat. Res., Vol.[**22**], (2007), 1322-1330.
6. **W.S. Choi, B.S. Jang, D.G. Lim, J. Yi, B. Hong,** Characterization of $Ba(Zr_{0.2}Ti_{0.8})O_3$ thin films deposited by RF-magnetron sputtering, J. Cryst. Growth, Vol.[**1**], (2002), 237–239.
7. **H. Chen, C. Yang, C. Fu, J. Shi, J. Zhang, W. Leng,** Microstructure and dielectric properties of $BaZr_xTi_{1-x}O_3$ ceramics, J Mater Sci: Mater Electron, Vol.[**19**], (2008), 379–382.
8. **N.S. Hari, T.R.N. Kutty,** Effect of secondary phase segregation on the positive temperature coefficient in resistance characteristics of n-$BaTiO_3$ceramics, J.Mater. Science, Vol.[**33**], (1998), 3275-3284.
9. **L.L. Kovalenko, O.I. V'yunov, A.G. Belous,** Semiconducting barium titanate doped with oxygen-free compounds, J. Eur. Cer. Soc, Vol.[**19**], (1999), 965-968.
10. **J.M. Millet, R.S.Roth, H.S.Parker,** Phase relations between the polytitanates of barium and the barium borates, vanadates, and molybdates, J.Am.Cer.Soc, 69, 811-814 (1986).
11. **In-Chyuan Ho,** Semiconducting barium titanate ceramics prepared by boron-containing liquid-phase sintering, J. Am. Cer. Soc, Vol.[**77**], (1994), 829-832.
12. **S.M. Rhim, S. Hong, H. Bak, O.K. Kim,** Effects of B_2O_3 addition on the dielectric and ferroelectric Properties of $Ba_{0.7}SR_{0.3}TiO_3$ Ceramics, J. Am. Cer. Soc., Vol.[**83**], (2000),1145-1148.
13. **J. Q. Qi, W. P. Chen, Y. Wang, H. W. Chan, L. T. Li,** Dielectric properties of barium titanate ceramics doped by B_2O_3 vapor, J. Appl. Phys., Vol.[**96**], (2004), 6937-6939.
14. **J. Q. Qi, Q. Zhu, Y. L. Wang, Y. J. Wu, and L. T. Li,** Enhancement of positive temperature coefficient resistance effect of $BaTiO_3$-based semiconducting ceramics caused by B_2O_3 vapor dopants, Solid State Commun., Vol.[**120**], (2001), 505-508.
15. **J. Q. Qi, Y. Wang, W. P. Chen, and H. L. W. Chan,** Effect of B_2O_3 vapor doping on the lattice parameter and electrical properties in $BaTiO_3$ ceramics, J. Appl. Phys., Vol.[**42**], (2003), L1516-L1518.
16. **J. Q. Qi, W. P. Chen, H. Y. Wang, L. T. Li, H. L. W. Chan,** Low temperature sintering behavior of B_2O_3 vapor in BaTiO3-based PTCR thermistors, Sens. Actuators, A **116**, (2004), 215-218.
17. **C. Ciomaga, M. Viviani, M. T. Buscaglia, V. Buscaglia, L. Mitoseriu, A. Stancu, P.Nanni,** Preparation and characterisation of the $Ba(Zr,Ti)O_3$ ceramics with relaxor properties, J. Euro. Cer. Soc., Vol.[**27**], (2007), 4061–4064.
18. **M. Sindhu, N. Ahlawat, S. Sanghi, R. Kumari, A. Agarwal**, Effect of Zr substitution on phase transformation and dielectric properties of $Ba_{0.9}Ca_{0.1}TiO_3$ ceramics J. of Applied Physics, Vol.[**114]**, (2013), 164106.
19. **C. A. Vasilescu, L.P. Curecheriu, L. Mitoşeriu, A. C. Ianculescu,** Phase formation, microstructure and functional properties of some $BaTi_{1-x}Zr_xO_3$ ceramics, U.P.B. Sci. Bull., Series B, Vol. [**77**], 1, (2015).
20. **L. Vuong, P.D. Gio, T.V. Chuong, D.T.H. Trang, D.V. Hung, N. T. Duong**, Effect of Zr/Ti ratio content on some physical properties of low temperature sintering PZT−PZN−PMnN

ceramics, International Journal of Materials and Chemistry, Vol.[**3**], 2, (2013), 39-43.

21. **S. Choudhury, S. Akter , M. J. Rahman, A. H. Bhuiyan S. N. Rahman, N. Khatun, M. T. Hossain,** Structural, dielectric and electrical properties of zirconium doped barium titanate perovskite, Journal of Bangladesh Academy of Sciences, Vol.[**32**], 2, (2008), 221-229.
22. **N. Abdelmoula, H. Chaabane, H. Khemakhem, R. von der mühll and A. Sımon,** Retraction: Relaxor or classical ferroelectric behavior in A site substituted perovskite type $Ba_{1-x}(Sm_{0.5}Na_{0.5})_x TiO_3$Phys. Stat. Sol. (A), Vol.[**203**], (2006), 987–996.
23. **S. Tsurekawa, K. Ibaraki, K. Kawahara, et al.,** The continuity of ferroelectric domains at grain boundaries in lead zirconate titanate, Scripta Mater. Vol.[**56**], 7, (2007), 557–580.
24. **S. Choudhury, Y.L. Li, C. Krill III, et al.,** Effect of grain orientation and grain size on ferroelectric domain switching and evolution: Phase field simulations, Acta Mater. Vol.[**55**], 4, (2007) 1415–1426.
25. **A. Toshihiro, K. Yasumasa,** Ferroelectric domain structures around the morphotropic phase boundary of the piezoelectric material $PbZr_{1-x}Ti_xO_3$, Phys. Rev. B 75 (2007) 214111.
26. **Wei Cai, Chunlin Fua, Jiacheng Gaob, Huaqiang Chen**, Effects of grain size on domain structure and ferroelectric properties of barium zirconate titanate ceramics, Journal of Alloys and Compounds, Vol.[**480**], (2009), 870–873.
27. **International Organization for Standard**, ISO 10545-3 (EN 99). Determination of water absorption, apparent porosity, apparent relative density and bulk density of ceramic tiles. Genebra; 1991.
28. **J. Bera, S. K. Rout,** On the formation mechanism of $BaTiO_3$ –$BaZrO_3$ solid solution through solid-oxide reaction, Mater. Lett. Vol.[**59**], (2005), 135-138.